http://dx.doi.org/10.5935/0103-5053.20130269

J. Braz. Chem. Soc., Vol. 25, No. 1, 65-74, 2014.
Printed in Brazil - ©2014 Sociedade Brasileira de Química
0103 - 5053 $6.00+0.00

Article

Effects of Na and K ions on the Crystallization of Low-silica X Zeolite and its Catalytic Performance for Alkylation of Toluene with Methanol

Haitao Hui,[a,b] Junhua Gao,[,a] Gencun Wang,[a,b] Ping Liu[a] and Kan Zhang*[,a]*

[a]*State Key Laboratory of Coal Conversion, Institute of Coal Chemistry, Chinese Academy of Sciences, 030001 Taiyuan, China*

[b]*University of Chinese Academy of Sciences, 100049 Beijing, China*

A cristalização da zeolita X com baixo teor de sílica (LSX) foi estudada em sistemas gelatinosos de Na-K, com diferentes graus de substituição do Na por K, enquanto fixou-se o conteúdo dos outros componentes. Difração de raios-X, espectroscopia de emissão atômica por plasma acoplado indutivamente, microscopia eletrônica de varredura, espectroscopia no infravermelho, e ressonância magnética nuclear foram usados para caracterizar as fases líquida e sólida. Na síntese do LSX, a relação molar de K/(Na+K) afetou a cristalização e a composição dos produtos finais. Uma maior fração molar do K correspondeu a uma menor taxa de cristalização, maior concentração de Si na fase líquida, e menor relação Si/Al do produto LSX obtido. O tamanho médio do LSX aumentou de forma constante com a substituição progressiva do Na por K nos géis originais, e a morfologia cristalina do LSX mudou gradualmente de volta para octaédrica. Na alquilação de tolueno com metanol sobre LSX, houve a diminuição da selectividade da alquilação do anel do produto xileno, enquanto que a alquilação na cadeia lateral dos produtos etilbenzeno e estireno aumentou com o aumento dos valores x exceto $x = 0$, devido à sua baixa cristalinidade.

The crystallization of low-silica X zeolite (LSX) was studied in Na-K gel systems with different extents of replacement of Na by K while fixed content of other components. X-ray diffraction, inductively coupled plasma atomic emission spectroscopy, scanning electron microscopy, infrared spectra, and nuclear magnetic resonance were used to characterize liquid and solid phase. In the synthesis of LSX, the molar ratio of K/(Na+K) affects the crystallization and the composition of final products. A higher mole fraction of K corresponded to a lower crystallization rate, higher concentration of Si in the liquid phase, and lower Si/Al ratio of the obtained LSX. The average size of LSX products steadily increased with the progressive replacement of Na by K in the initial gels, and crystal morphology of the LSX products gradually changed from round to octahedral. For alkylation of toluene with methanol over obtained LSX, the selectivity of ring alkylation product xylene decreased while the side chain alkylation products styrene and ethylbenzene increased with the increased x values except $x = 0$, which was due to its low crystallinity.

Keywords: LSX, synthesis, Na, K, Alkylation

Introduction

Zeolite X is a kind of microporous material with a faujasite framework structure and a Si/Al molar ratio that varies from 1.0 to 1.5. Each unit cell in the three-dimensional pore system of faujasite zeolite consists of 8 supercages, 8 sodalite cages, and 16 hexagonal prisms.[1] Zeolite X is receiving increased attention because of its prominent selective adsorption property,[2-4] high exchange capacity[5] and medium-strength basic sites.[6,7] Kim *et al.*[2] studied the adsorption characteristics of nitrogen and oxygen with Li^+ and H^+ co-exchanged LSX (Li-H-LSX). They found that Li-H-LSX has higher nitrogen capacity and selectivity, and that it could be used as selective nitrogen adsorbent for air separation. Regarding ion exchange, the change rate to hydrated magnesium ion is five times higher than zeolite 4A.[5] Given that LSX has appropriate acidity, basicity, and suitable acid-base pair sites, it can be used to catalyze the side chain alkylation of toluene with methanol to synthesize styrene.[6-8] Alkylation of toluene with methanol over LiX, NaX, KX, RbX and CsX yields different products, either xylene or styrene and ethylbenzene, depending on whether

*e-mail: gaojunhua@sxicc.ac.cn, zhangkan@sxicc.ac.cn

ring alkylation or side chain alkylation is favored.[9] It has been observed that ring alkylation of toluene by methanol to give xylene is favored on relatively high acidic zeolites like LiX and NaX, while side chain alkylation to give styrene and ethylbenzene is favored on basic zeolites like KX, RbX and CsX.[10]

Aluminosilicate zeolites are usually synthesized under basic conditions; thus, cations are inducted together with OH^-. Cations remarkably affect the properties of the aluminosilicate gel and the forms of the zeolite framework because of their "structure-forming" or "structure-breaking" capacities.[11] Hydrothermal synthesis method in the Na-K system is a common way to synthesize zeolite X.[12-14] Previous work studied the synthesis of LSX zeolite from kaolin clays heated with sodium carbonate in highly alkaline-mixed Na/K hydrothermal systems. They investigated the effect of the Na/K ratio on both the crystallization reaction and the characteristics of the products thus obtained.[14] However, they did not investigated the effects of different Na/K ratios on the chemical compositions of liquid and solid phases in the synthesis process, and not explained why K replacing Na could affect crystal products. Therefore, the effect of replacing Na by K in the synthesis of LSX should be further investigated to aid the development of LSX.

This study investigated the effect of K/(Na+K) molar ratio in the synthesis of LSX. Focused was given on the effects of varying the amounts of K replacing Na on the crystallinity, crystallization rate, crystal morphology, crystal size and distribution of the LSX products, as well as on the chemical composition of the liquid and solid phases in Na-K system. At last, the catalytic behaviors of LSX products for the alkylation of toluene with methanol were discussed.

Experimental

Reagents

Sodium hydroxide (NaOH), potassium hydroxide (KOH), sodium metaaluminate ($NaAlO_2$), and sodium silicate ($Na_2SiO_3{\cdot}9H_2O$) were used to synthesize LSX. All reagents were analytical grade. Distilled water was used throughout.

Gels preparation

LSX was synthesized by varying the molar ratios of $K_2O/(Na_2O+K_2O)$ with the molar ratios of $(Na_2O+K_2O)/Al_2O_3$, SiO_2/Al_2O_3, and H_2O/Al_2O_3 held constant. No interferences from other cations and anions (except the required ions Na^+, K^+, Al^{3+}, $[SiO_3^{2-}]_n$, and OH^-) in the initial gel and solution throughout the entire synthesis process. Gels with the following oxide molar compositions were prepared for LSX synthesis:

$$5.5[(1–x)Na_2O{:}xK_2O]{:}Al_2O_3{:}2.2SiO_2{:}260H_2O$$

where $x = K_2O/(Na_2O+K_2O) = K/(Na+ K)$, defined as the extent of Na replacement by K. The x values were varied from 0 to 0.4 by adding appropriate amounts of NaOH and KOH.

First, m g NaOH, n g KOH (Table 1) and 8.20 g $NaAlO_2$ were dissolved in 110.00 g H_2O together, and 31.25 g $Na_2SiO_3{\cdot}9H_2O$ was dissolved in 106.50 g H_2O at 50 °C. Then, two kinds of solutions above were mixed at 50 °C and made into gels in the synthesis reactor.

Table 1. Contents of NaOH and KOH for the LSX synthesis

x	0	0.1	0.2	0.3	0.4
m	9.20	7.00	4.80	2.60	0.40
n	0.00	3.09	6.17	9.26	12.34

LSX was also synthesized in the pure Na system by increasing the content of NaOH without KOH while keeping the molar ratios of SiO_2/Al_2O_3, and H_2O/Al_2O_3 constant. Gels with the following oxide molar compositions were prepared for LSX synthesis:

$$yNa_2O{:}Al_2O_3{:}2.2SiO_2{:}260H_2O$$

where y ranges from 5.5 to 6.2.

First, w g NaOH (Table 2) and 8.20 g $NaAlO_2$ were dissolved in 110.00 g H_2O together, and 31.25 g $Na_2SiO_3{\cdot}9H_2O$ was dissolved in 106.50 g H_2O at 50 °C. Then, two kinds of solutions above were mixed at 50 °C and made into gels in the synthesis reactor.

Table 2. Content of NaOH for the LSX synthesis

y	5.5	5.6	5.7	5.8	5.9	6.0	6.1	6.2
w	9.20	9.60	10.00	10.40	10.80	11.20	11.60	12.00

Synthesis of LSX

LSX was synthesized by a two-step hydrothermal process. The gels prepared above were aging at 50 °C for 24 h and crystallizing at 100 °C for different durations indicated in the following text using homogeneous synthesis reactors with stirring at 30 rpm. After cooling the reactors, the samples were centrifuged at 3000 rpm,

and the liquid phase was collected to analyze the chemical composition. Afterwards, the recovered solid product was washed until pH 7.0 and dried at 100 °C. After each run, the PTFE reactors were soaked with HCl (aq.) and washed with distilled water to clean out residual seed crystals.

Characterization and catalytic test

Powder X-ray diffraction (XRD) with Cu Kα radiation was carried out to determine the crystallinity of the solid products. The scanning range (2θ) was set between 5° and 50° with a step size of 0.02°. Inductively coupled plasma atomic emission spectroscopy (ICP-AES) (Thermo iCAP 6300) was performed to determine the concentrations of elements in liquid and solid phases. Scanning electron microscopy (SEM) (Sirion200) was used to observe crystal size and morphology. Infrared (IR) spectra of zeolite products from 400 cm^{-1} to 1400 cm^{-1} were recorded on a Nicolet 380 FT-IR using the KBr pellet technique. Both ^{29}Si and ^{27}Al magic angle spinning nuclear magnetic resonance (MAS NMR) spectra were measured with an AVANCE AV 400 spectrometer. Both CO_2 and NH_3 temperature programmed desorption (CO_2-TPD and NH_3-TPD) were used to determine the basic and acid strengths of LSX products.

The catalytic tests of LSX products obtained for the alkylation of toluene with methanol (toluene/methanol molar ratio = 5) were carried out in a fixed-bed reactor at 425 °C with a mass space velocity of 1 h^{-1}. LSX products were pressed, crushed, and sieved to 40-60 mesh. The samples (6.0 g) were placed in a quartz tube with an inner diameter of 10 mm. Reaction was conducted at atmospheric pressure. The obtained alkylation products were analyzed by a gas chromatography (SP3420) with Inowax capillary column. The conversions of the raw materials (C(i)) and the Selectivity of the products (S(j)) were defined as follows:

$$C(\mathrm{i}) = \frac{\text{The mole number of the consumed material i}}{\text{The mole number of the feed material i}}$$

$$S(\mathrm{j}) = \frac{\text{The molar number of the product j}}{\text{The mole number of the consumed methanol}}$$

Results and Discussion

Crystallization kinetics

Figure 1 shows the XRD patterns of the solid phase for different x values of crystallizating for 6 h. The peaks at 6.1°, 10.0°, 15.4°, 23.3°, 26.6°, and 30.9°, i.e., the characteristic peaks of zeolite with a faujasite structure[15] were observed on the XRD patterns of all the solid samples. This is in agreement with standard spectra of NaX (JCPDS No. 38-0237). When the Si/Al ratio is lower than 1.15, the X zeolite is usually called LSX.[16] Combining the powder XRD patterns with the Si/Al molar ratio in Table 3, we can conclude that the LSX products were obtained under the synthesis conditions described above except x = 0.

Table 3. Silicon aluminum ratios of LSX products at different x values (crystallization time = 6 h)

x (K/(Na + K))	Si/Al(bulk)	Si/Al(framework)
0	1.21	1.22
0.1	1.16	1.16
0.2	1.14	1.15
0.3	1.13	1.14
0.4	1.12	1.14

Si/Al(bulk): total silicon aluminum ratio of solid phase, from ICP-AES; Si/Al(framework): skeleton silicon aluminum ratio of LSX, from ^{29}Si NMR.

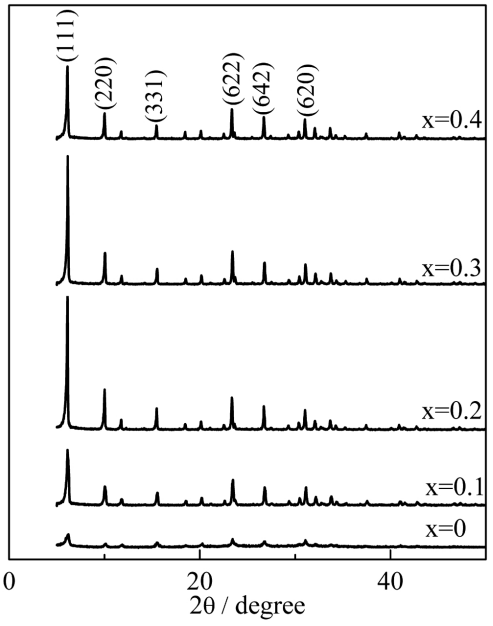

Figure 1. XRD patterns of the solid phase at different x values (crystallization time = 6 h).

Standard X-type zeolite was synthesized according to reference[12] and the intensity of the characteristic peaks at 6.1°, 10.0°, 15.4°, 23.3°, 26.6°, and 30.9° [15] were recorded as crystallinity reference. The crystallization results are shown in Figure 2. It is observed that the crystallinity is lower when $x = 0$, while pure X-type zeolite can be obtained when $x = 0.1$, $x = 0.2$, $x = 0.3$, and $x = 0.4$. Crystallization curves plotted in Figure 2 show the complex influence of x on the crystallization kinetics. As can be seen from it, an optimum crystallization time was required for each x to get LSX product with higher crystallinity, and the

crystallization rate decreased gradually from x = 0 to x = 0.4. The highest crystallinity can be achieved when crystallization times were as follows: 5 h at x = 0 and x = 0.1, 6 h at x = 0.2 and x = 0.3, 7 h at x = 0.4. After the optimum crystallization time, the crystallinity decreased gradually at each x and the solid phases turned to gels gradually.

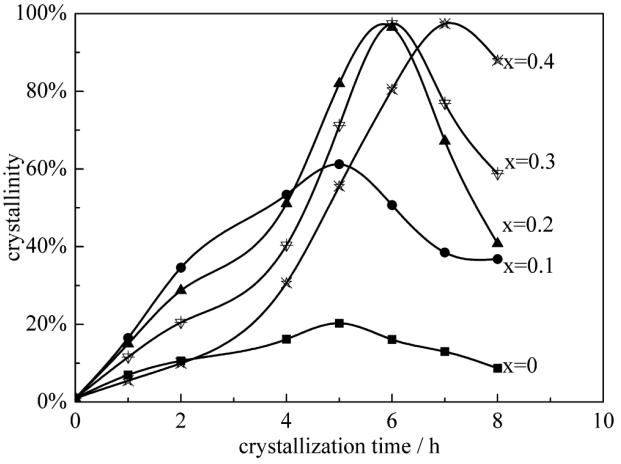

Figure 2. Crystallinity of LSX products as a function of crystallization time for each x values.

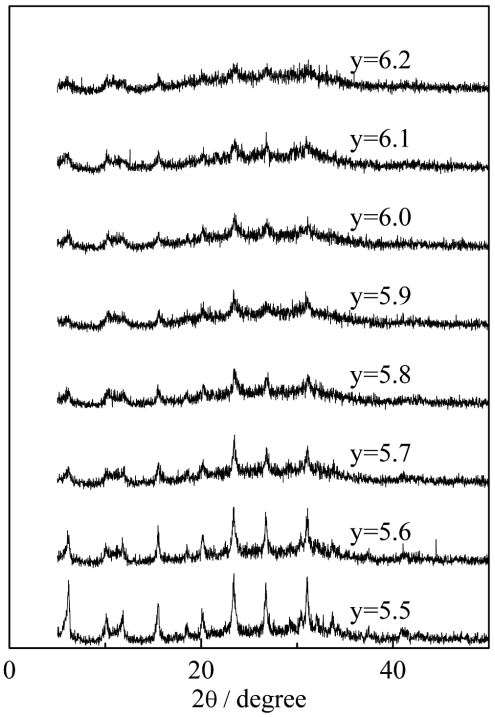

Figure 3. XRD patterns of the solid phase for different y values (crystallization time = 5 h).

For x = 0, the crystallinity of the solid product was very low. In order to prove that the effect of K replacing Na for synthesis of LSX is not that the alkali strength of KOH is stronger than NaOH in the same concentration, LSX was also synthesized by increasing the content of NaOH without KOH while keeping the molar ratios of SiO_2/Al_2O_3, and H_2O/Al_2O_3 constant. Figure 3 shows the XRD patterns of the solid phase with different y and crystallization for 5 h. Crystallinity was low for y = 5.5, 5.6, and 5.7. When the NaOH content continuously increased (above 5.7), LSX was hardly synthesized and the products were mostly gel. The reason could be that the basicity of the alkali solutions was so strong that the LSX crystal could be resolved in them. Therefore, LSX cannot be synthesized in a solution with low initial Si/Al molar ratio, sodium-containing, and no potassium under the synthesis condition of aging at 50 °C for 24 h and crystallization at 100 °C for a few hours.

Crystal morphology and size distribution

The SEM images of LSX products obtained at x = 0.4 throughout the crystallization process are shown in Figure 4. The SEM image of LSX product in the initial time (0 h) shows that the solid product had an extreme rough surface, which suggested that the product contained quite amount of amorphous phase and the crystallinity was low. The grains were appeared and grew gradually in the whole crystallization process. A certain amount of grains with the size of 3 μm could be synthesized at 4 h, though their surface was rough. Remarkably the grains with smooth surface and octahedral morphology could be got at 7 h, which suggests that the product has high crystallinity. The result is agreed with the products crystallinity (Figure 2).

The SEM images of LSX products obtained at different x values are shown in Figure 5. The SEM image of LSX product for pure Na gel (x = 0) shows that the solid product had an extreme rough surface, which suggested that the product contained quite amount of amorphous phase and the crystallinity was low. The result is agreed with the XRD pattern (Figure 1). Remarkably the crystal morphology at x = 0.4 was almost octahedral shape and had very smooth surface. As can be seen from Figure 5, the replacement of Na by K gradually changed the crystal morphology of the solid products from round to octahedral.

The crystal size distributions were shown in Figure 6. The crystal size distribution range was broad when the replacement of Na by K was low (x = 0.1). When the replacement was higher (x = 0.4), the crystal size distribution becomes narrow, and most of the crystal particles were approximately 3.0 μm. The results suggests that the crystal size distribution becomes narrow (Figure 6) and the average size of the crystal products steadily increased with the increased replacement of Na by K in the initial gels. The reason was probably that K^+ plays a role of structure breaking ions,[17] thus the number of nuclei

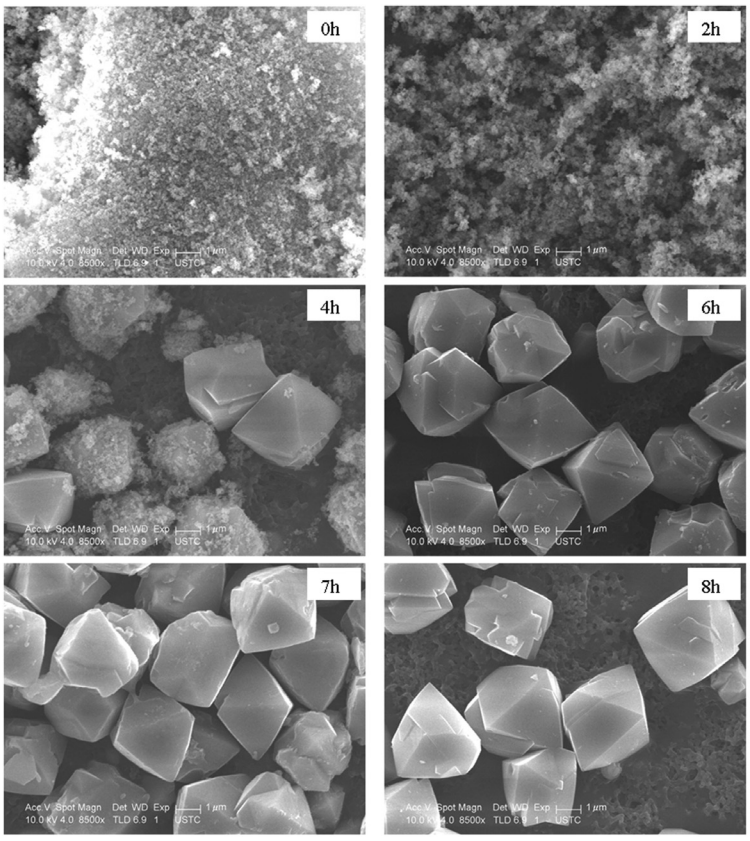

Figure 4. SEM images of the LSX products obtained at $x = 0.4$.

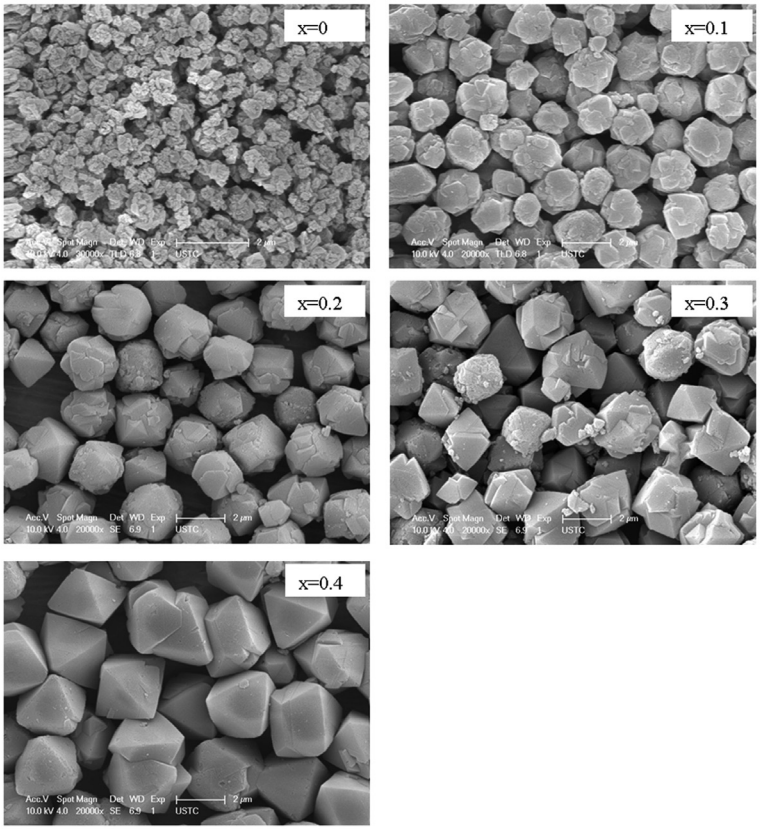

Figure 5. SEM images of the LSX products obtained at different x value (crystallization time = 6 h).

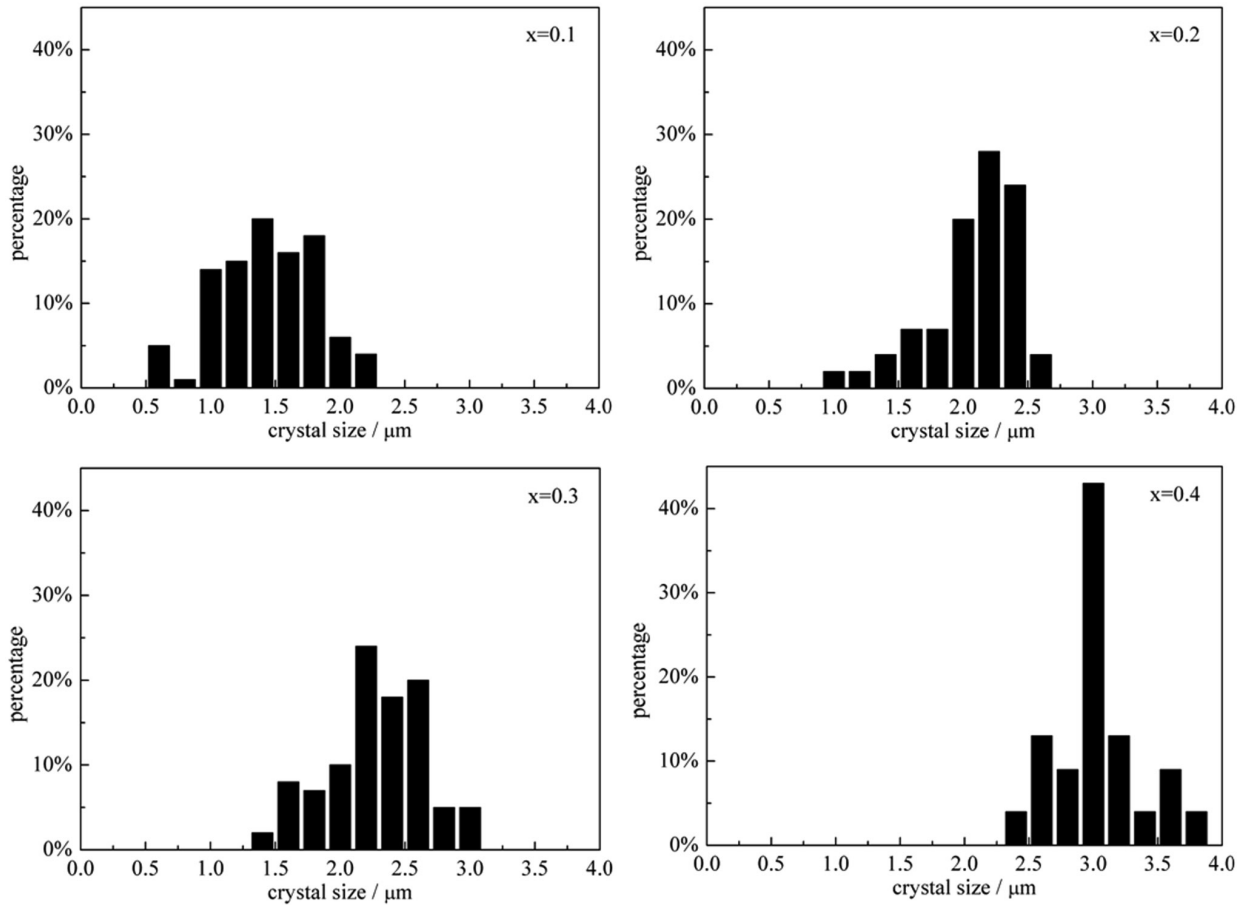

Figure 6. Crystal size distributions of the LSX products at different *x* values (crystallization time = 6 h).

formed in gel matrix decreased with the increase of the fraction of K^+, which leads the growth of nuclei become more predominant compared with the nucleus formation during the synthesis process of LSX.

^{29}Si and ^{27}Al NMR spectra of LSX products

Figure 7(a) shows the ^{29}Si NMR spectra of LSX products obtained after crystallization for 6 h. The peaks at –103, –99, –94, –89, and –85 ppm were assigned to Si atoms having 0, 1, 2, 3, and 4 Al atoms respectively in their second coordination sphere indicated as Si(0Al), Si(1Al), Si(2Al), Si(3Al), and Si(4Al), respectively.[18] As shown in Figure 7(a), the peak area at −85 ppm was much larger than the others, and the peak areas at −103 and −99 ppm were almost zero, which indicated that Si atoms are almost linked with Al atoms through O atoms in the zeolite framework.

Figure 7(b) shows the ^{27}Al NMR spectra of the LSX products obtained after crystallization for 6 h. At each *x*, the ^{27}Al NMR spectra only showed one peak centered at 62 ppm, which belongs to tetrahedral Al (IV) species,[18] whereas the octahedral Al (VI) is almost nonexistent (the peak at 0 ppm).

The Si/Al molar ratio of the zeolite framework can be calculated from ^{29}Si NMR spectra according to the equation 1,[18] and the results are shown in Table 3. There is no significant difference between Si/Al(bulk) and Si/Al(framework) for each *x*. This finding indicated that the relative contents of Si and Al incorporated into the gel and crystal were approximately the same in same crystallization time. The Si/Al ratios of the obtained LSX also decreased with increased initial K/(K + Na) ratio. This phenomenon can be explained as below.

$$\frac{n_{Si}}{n_{Al}}(framework) = \frac{\sum_{n=0}^{4} I_{Si(nAl)}}{\sum_{n=0}^{4} \frac{n}{4} I_{Si(nAl)}} \quad (1)$$

Crystallization process: chemical compositions of liquid and solid phases

The chemical compositions of liquid and solid phases are collected in Figure 8 and Figure 9 respectively. The experimental data showed that the contents of sodium and potassium decreased in the liquid and increased in the solid phases slightly in the initial crystallization process.

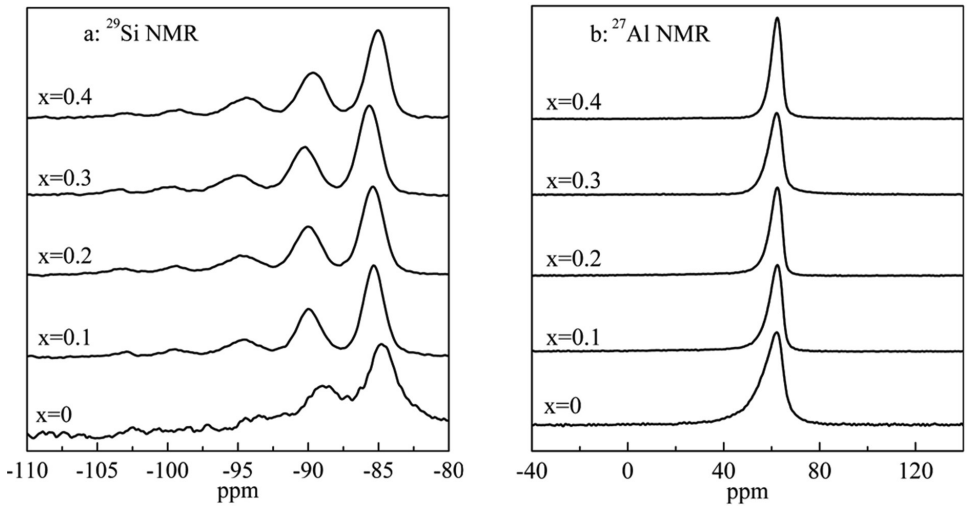

Figure 7. ^{29}Si and ^{27}Al NMR spectra of the LSX products (crystallization time = 6 h).

The amount of aluminum in the liquid phase decreased at the beginning of the crystallization process and almost remained constant after crystallinity reached the maximum. The amount of silicon in the liquid phase slightly increased at the beginning of the crystallization process and almost remained constant thereafter.

In strong alkaline solutions, silicon mostly exists as the monomeric silicate species,[19] and aluminum exists as $Al(OH)_4^-$ species in the liquid phase during the synthesis process of LSX.[20] In the initial gel, silicon combined with silicon or aluminum into amorphous gels and transformed into solid phase. With the increased initial K/(Na+K) ratio,

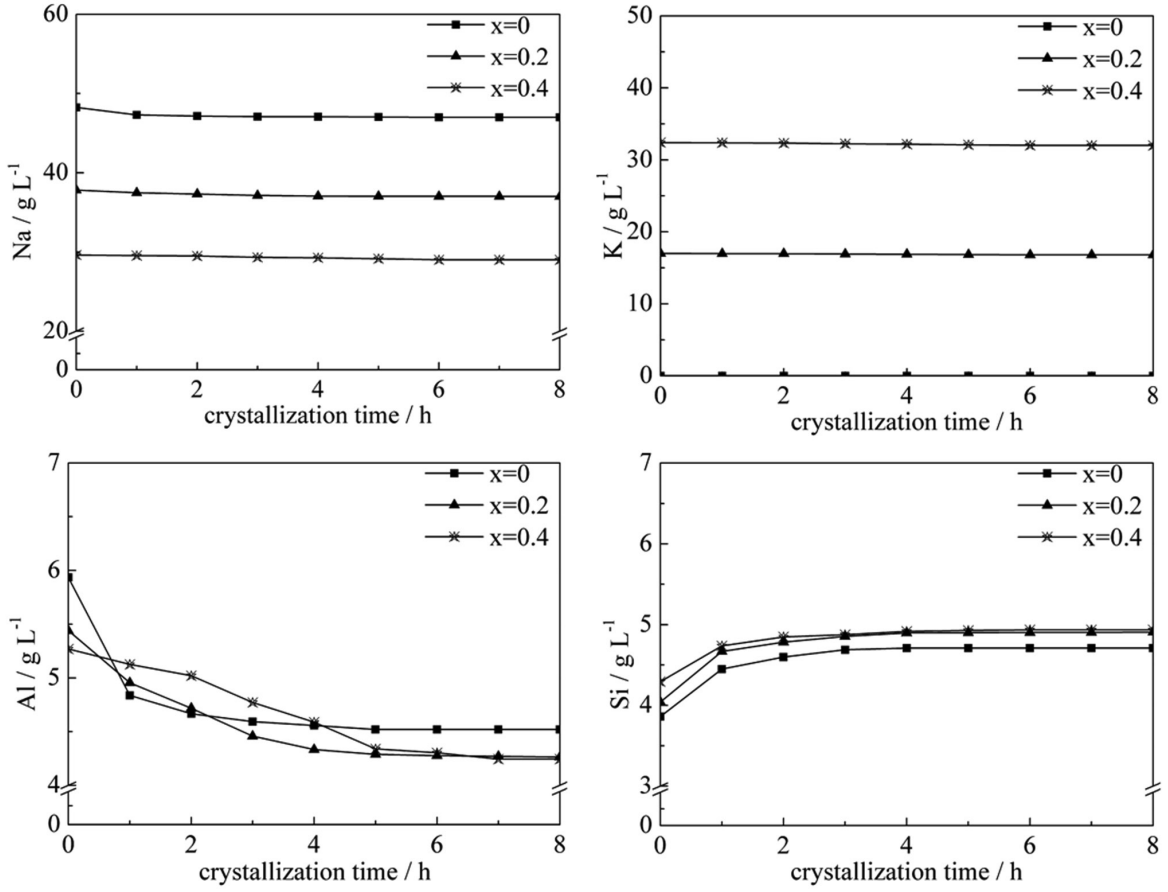

Figure 8. Contents of Na, K, Si and Al in the liquid phase.

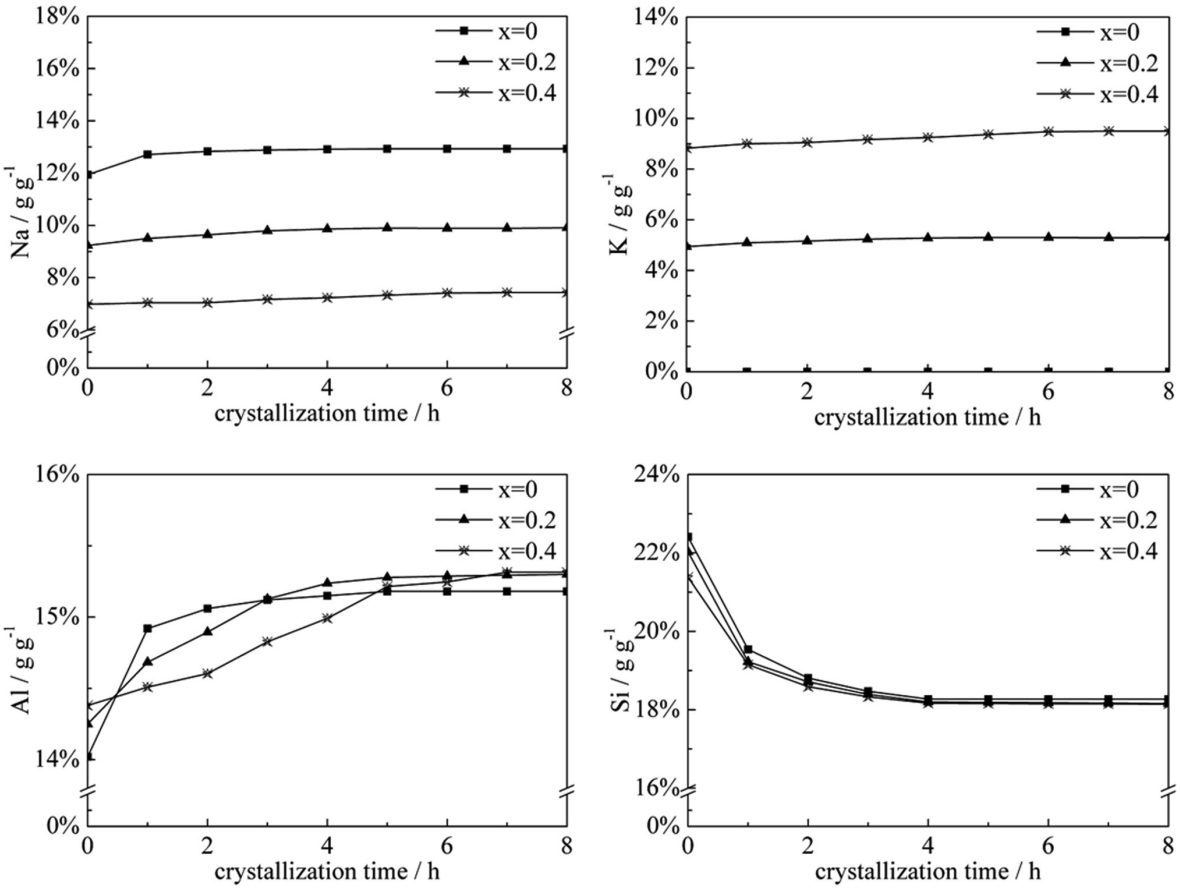

Figure 9. Contents of Na, K, Si and Al in the solid phases.

the pH of liquid solution increased, and the combination strength between silicon and silicon decreased. Therefore the content of silicon in the solid phase decreased with the increased *x* values in the same crystallization time. The concentration of silicon in the liquid phase increased with the increased crystallization time for all *x* values, which is caused by the dissolution of amorphous aluminosilicate during the heating of the reaction mixture from aging temperature (50 °C) to crystallizing temperature (100 °C).

The content of aluminum in the solid phase during the LSX crystallization process shows rather complex dependence on *x* and crystallization time. As can be seen in Figure 9, the content of aluminum increased with the increased *x* values in the initial crystallization stage and after pure LSX products were obtained. Besides, the increase rate of aluminum content in the solid phase decreased with the increased *x* values during the LSX crystallization process, which is in accord with the changes of crystallization rate.

The content of silicon decreased and the content of aluminum increased in the solid phase with the increased *x* values after pure LSX products were obtained. It indicated that the Si/Al ratio of zeolite products decreased with the increased *x*. This can be confirmed by IR spectra. The IR spectra of LSX products at different *x* values are shown in Figure 10. A band at around 1080 cm^{-1} was assigned to the asymmetric stretching vibration of the Si–O bond[21] in the framework of LSX. At different *x* values, the asymmetric stretching vibration of Si–O bond ($\nu_{as(Si-O)}$) slightly differed, as shown in Figure 10. The peak of the asymmetric stretching vibration of Si–O bond shifted to low wave numbers slightly with increased *x* values. This finding indicates that the Si–O bond in the framework of the LSX weakened because the oxygen atoms of the Si–O bond combined with aluminum atoms. Hence, more aluminum atoms were incorporated into the framework of zeolite and the Si/Al ratio of zeolite products decreased with the increased *x*.

Catalytic behaviors of LSX products for the alkylation of toluene with methanol

The results of the catalytic performances of the obtained LSX products for the alkylation of toluene with methanol were shown in Table 4. As can be seen from it, the main products were carbon monoxide and hydrogen, though a

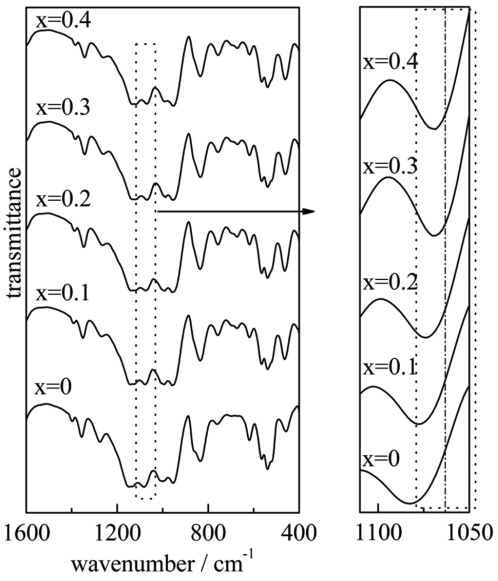

Figure 10. IR spectra of the LSX products at different *x* values (crystallization time = 6 h).

certain amounts of xylene, ethylbenzene and styrene were generated.

The selectivity of styrene and ethylbenzene increased with the increased *x* values from 0 to 0.4. The CO_2-TPD spectra (Figure 11(a)) showed that all LSX products obtained at different *x* values presented a major peak at relatively low temperature (around 220 °C), which corresponded to the basic sites. The peaks slightly shifted to high temperatures with increased *x* values, which indicated that the base strength of the LSX products gradually increased with increased *x* values. This could be attributed the fact that the charge-to-radius of potassium ion is lower than sodium ion, which leads the base strength of lattice

Table 4. Results of the alkylation of toluene with methanol over LSX products (crystallization time = 6 h)

x		0	0.1	0.2	0.3	0.4
$C_{methanol}$ (%)		50.26	69.18	70.08	72.26	75.18
$S_{styrene+ethylbenzene}$ (%)		1.29	1.56	1.91	1.99	2.06
S_{xylene} (%)	*para-*	2.36	4.90	4.78	4.05	3.33
	meta-	2.03	3.86	3.64	3.09	2.50
	ortho-	5.32	11.06	10.92	9.40	7.63
$S_{carbon\ monoxide}$ (%)		88.78	78.39	78.50	81.24	84.26
$S_{methane+trimethylbenzene+others}$ (%)		0.22	0.26	0.25	0.23	0.22

oxygen become stronger. While the side chain alkylation of toluene with methanol to give styrene and ethylbenzene was favored on relatively more basic zeolites to some extent. Besides, methanol could be decomposed to carbon monoxide and hydrogen over the more basic sites of the LSX, therefore, the conversion of methanol becomes higher with increased *x* values.

The highest selectivity of xylene can be obtained at $x = 0.1$. The NH_3-TPD spectra (Figure 11(b)) showed that all LSX products obtained at different *x* values presented a major peak at relatively low temperature (around 240 °C), which corresponded to the acidic sites. The peaks slightly shift to a low temperature with increased *x* values from 0.1 to 0.4 except $x = 0$. This finding indicated that the acidity strength of the LSX products gradually decreased with increased *x* values. While the ring alkylation of toluene with methanol to give xylene was favored on relatively high acidic zeolites, therefore the selectivity of xylene decreased with the increased *x* values except $x = 0$. At $x = 0$, the acidity strength of LSX product was the weakest, and the selectivity

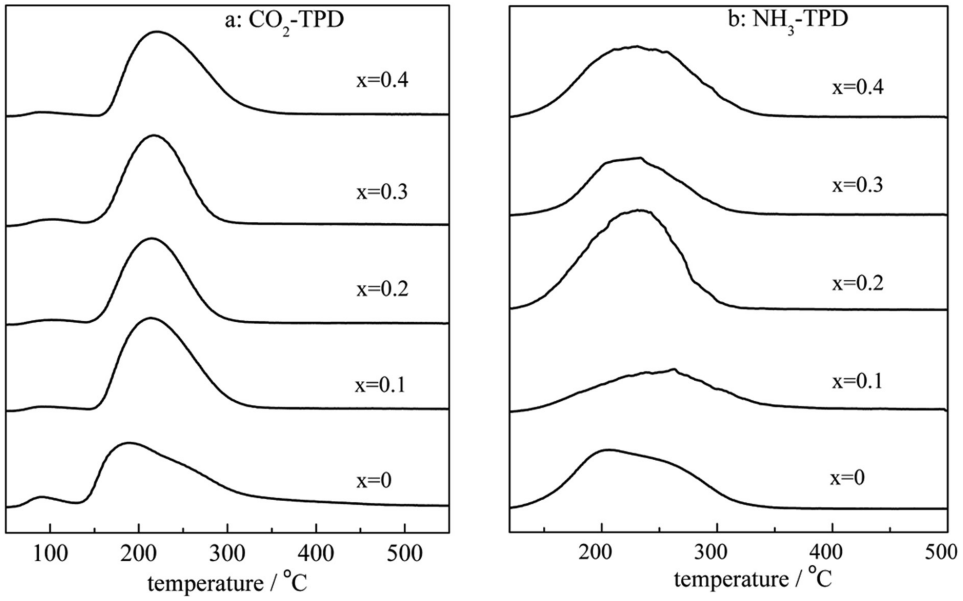

Figure 11. CO_2-TPD and NH_3-TPD spectra of LSX products obtained at different *x* values (crystallization time = 6 h).

of xylene or styrene and ethylene were very lower. These results can be due to its low crystallinity

Conclusion

The crystallization rate, crystal size and distribution, crystal morphology, as well as chemical composition depended on the mole fraction of K in the Na-K system during the synthesis of LSX. A higher mole fraction of K in the initial gels resulted in lower crystallization rate, and lower framework Si/Al ratio in the LSX obtained. The average size of the LSX products steadily increased with the progressive replacement of Na by K in the initial gels, and the crystal morphology of the solid products gradually changed from round to octahedral.

For alkylation of toluene with methanol over the obtained LSX, the main products were xylene, styrene, and ethylbenzene. The selectivity of ring alkylation product xylene decreased with the increased x values because of the decreased acidity strength of the LSX products. The selectivity of side chain alkylation products styrene and ethylbenzene increased with the increased x values because of the increased base strength of the LSX products. The selectivity of all products were low when $x = 0$, which was due to its low crystallinity.

References

1. Eulenberger, G. R.; Shoemake, D. P.; Keil, J. G.; *J. Phys. Chem.* **1967**, *71*, 1812.
2. Kim, J. B.; *Korean Chem. Soc.* **2003**, *24*, 1814.
3. Kim, H. S.; Ko, S. O; Lim, W. T.; *Bull Korean Chem. Soc.* **2012**, *33*, 3303.
4. Guesmi, H.; Massiani, P.; Nouali, H.; Paillaud, J. L.; *Microporous Mesoporous Mater.* **2012**, *159*, 87.
5. Li, Z. L.; Zhi, J. P.; Zhang, W.; Hu, Q. X.; Zhang, Y. L.; *J. Chin. Ceramic Soc.* **2008**, *36*, 246.
6. Hunger, M.; Schenk, U.; Seiler, M.; Weitkamp, J.; *J. Mol. Catal. a-Chem*. **2000**, *156*, 153.
7. Fan, F.; Feng, Z.; Li, G.; Sun, K.; Ying, P.; Li, C.; *Chem. Eur. J.* **2008**, *14*, 5125.
8. Borgna, A.; Sepúlveda, J.; Magni, S. I.; Apesteguía, C. R.; *Appl. Catal., A*. **2004**, *276*, 207.
9. Serra, J. M.; Corma, A.; Farrusseng, D.; Baumes, L.; Mirodatos, C.; Flego, C.; Perego, C.; Catal. *Today* **2003**, *81*, 425.
10. Sivasankar, N.; Vasudevan, S.; *J. Indian Inst. Sci.* **2010**, *90*, 231.
11. Aiello, R.; Crea, F.; Anastro, I.; Subotić, B.; Testa, F.; *Zeolites* **1991**, *11*, 767.
12. Kühl, G. H.; *Zeolites* **1987**, *7*, 451.
13. Akolekar, D.; Chaffee, A.; Howe, R. F.; *Zeolites* **1997**, *19*, 359.
14. Basaldella, E. I.; Tara, J. C.; *Zeolites* **1995**, *15*, 243.
15. Fan, F. T.; Feng, Z. C.; Li, G. N.; Sun, K. J.; Ying, P. F.; Li, C.; *Chem.-Eur. J.* **2008**, *14*, 5125.
16. Daems, I.; Leflaive, P.; Methivier, A.; Baron, G. V.; Denayer, J. F. M.; *Microporous Mesoporous Mater*. **2006**, *96*, 149.
17. Bronic, J.; Jelic, T. A.; Krznaric, I.; Kontrec, J.; Subotic, B.; Mali, G.; *Acta Chim. Slov.* **2008**, *55*, 918.
18. Xu, R.; Pang, W.; Yu, J.; Huo, Q.; Chen, J.; *Beijing: Science Press*. **2004**, 168.
19. Dutta, P. K.; Shieh, D. C.; Puri, M.; *J. Phys. Chem.* **1987**, *91*, 2332.
20. Xiong, G.; Yu, Y.; Feng, Z.; Xin, Q.; Xiao, F.; Li, C.; *Microporous Mesoporous Mater*. **2001**, *42*, 317.
21. Jung, K. Y.; Park, S. B.; *Appl. Catal. B-Environ.* **2000**, *25*, 249.

Submitted: September 3, 2013
Published online: November 13, 2013